Nigerian Journal of Technology (NIJOTECH)
Vol. 41, No. 1, January, 2022, pp.8 –20
www.nijotech.com

Print ISSN: 0331-8443
Electronic ISSN: 2467-8821
http://dx.doi.org/10.4314/njt.v41i1.2

Application of Variation Method in Three Dimensional Stability Analysis of Rectangular Plate Using Various Exact Shape Functions

F. C. Onyeka[1,3], B. O. Mama[2,] *, C. D. Nwa-David[3]

[1]*Department of Civil Engineering, Edo State University, Uzairue, Edo State, NIGERIA.*
[2]*Department of Civil Engineering, University of Nigeria, Enugu State, NIGERIA*
[3]*Department of Civil Engineering, Michael Okpara University of Agriculture, Umudike, Abia State, NIGERIA*

Abstract
In this paper, a polynomial and trigonometric shape function are developed for the three-dimensional (3-D) stability analysis of a thick rectangular plate. This study has evaluated the effect of aspect ratio of the critical buckling load of a plate that is clamped on the first edge, free at the third edge, with the second and fourth edges simply supported respectively (CSFS) using a variational method. An expression of potential energy of thick plate was formulated using 3-D elastic principles thereafter, a compatibility equation of 3-D plate was derived through energy equation transformation to get the relations between the rotations and deflection. The solution of compatibility equations yields the exact plates shape function which is derived in terms of trigonometric and polynomial displacement and rotations. Similarly, by minimizing the energy equation with respect to the deflection, the direct governing equation was formulated. The solution of governing equation yields the deflection coefficient of the plate. By minimizing the potential energy equation with respect to deflection coefficient after the action deflection and rotations equation were substituted into it, a more realistic formula for calculation of the critical buckling load is established. The proposed method unlike the refined plate theory (RPT), considered all the six stress elements in the analysis. The result showed that the critical buckling loads from the present study using polynomial are slightly higher than those obtained using trigonometric theories signifying the more exactness of the latter. The result of the present study using the established 3-D model for both functions is satisfactory and closer to exact solution compared to the two- dimensional (2-D) RPT. The overall average percentage differences between the two functions recorded are 6.4%. This shows that at about 94% both approaches are the same and can be applied with confidence in the stability analysis of any type of plate with the boundary condition.

Keywords: Uniaxial buckling, CSFS rectangular plate, compressive load, variational method, stability analysis of thick plate, three-dimensional (3-D) plate theory.

1.0 INTRODUCTION

A plate is a solid that consists of two parallel plane surfaces separated by a small dimension called thickness [1, 2]. Compared with the thickness, the planer surface dimensions are large. Based on shapes, plates can be rectangular, square, triangular circular, elliptical, circular with hole, or square with hole. They can also be isotropic, anisotropic, orthotropic, homogeneous, and heterogeneous, regarding the materials of construction. Based on weight, plates can be thin or thick [3, 4]. At the edges, plates have varying boundary conditions; for a rectangular plate, they are clamped support, simply supported and free edged.

Plates are three dimensional structural elements widely used in architectural structures and various engineering applications such as floor slabs, bridge decks, rigid pavements of highways and airport runways, ship decks, aircraft and spacecraft panels and retaining walls. Plates can exhibit flexural, dynamic, as well as buckling behaviors and the behavior of plates depends on the type and nature of load application [5, 6].

In the design of engineering structures, stability is a factor of great importance that must be considered and it is especially true for structures with one or two dimensions that are small in relation to the other dimensions, such as plates. Instability of structures is commonly characterized with buckling [7]. A structure is said to buckle when it encounters large deformation and loses its ability to withstand the load at a critical load value. Buckling of plates can be analyzed using numeric, equilibrium or energy methods [8, 9]. With the increased use of thick plates in engineering projects, stability analysis of plate structures is required. Meanwhile, considering different

***Corresponding author **(Tel:** +234 (0) 8035706531**)**
Email addresses: *onyeka.festus@edouniversity.edu.ng* (F. C. Onyeka), *benjamine.mama@unn.edu.ng* (B.O Mama), *nwadavid.chidobere@mouau.edu.ng* (C.D Nwa-David)

methods of analysis, unlike 2-D, more attention has not been channeled to typical 3-D plate analysis approach because of their rigorous mode of analysis as they considered all the stress element in the analysis.

2.0 LITERATURE REVIEW

The analysis of plates has attracted great research interest with many varying methods being developed and applied. Considering the insufficient ability of plates towards withstanding compressive forces in structures carrying in-plane compressive loads, the necessity of stability analysis is undeniable.

For a rectangular thin plate with two simply supported edge, one clamped and free support edge (SSCF) and all edges simply supported plate (SSSS) subjected uniaxial uniform compressive loads, single finite Fourier sine integral transform method was used by Onyia *et al.* [10] to solve the problem of elastic stability. A thick plate as well as variational method was not considered by the authors. Also, the authors did not consider CSFS boundary condition.

Onwuka *et al.* [11] used the Galerkin's method to analyze buckling in an all-edge simply supported thin rectangular isotropic plates. Polynomial series was used to obtain the plate equation of deflection. Although the energy approach was used, the authors did not consider trigonometric functions for their buckling analysis, neither was a thick plate with CSFS boundary condition considered.

Ibearugbulem *et al.* [12] carried out a study on the buckling analysis of axially compressed rectangular plate by using Taylor-Mclaurin's series in its theoretical formulation, thereafter, Ritz approach was applied to determine the numerical field of unknown function of thin rectangular flat SSSS plate. They did not consider a thick plate for their buckling analysis and did not derive the expression from the governing equation rather, the shape function used was assumed, thereby making their result not a close-form solution and cannot be used to solve plate problems with CSFS boundary condition and that other heavy type of plates.

Sayyad and Ghugal [13] studied the buckling load analysis in a thick isotropic plate which was subjected to biaxial and uniaxial in-plane forces, by applying shear exponential deformation theory. The simply supported thick isotropic square plates were considered in the detailed numerical studies. Although a thick plate, the authors did not consider a thick plate with CSFS boundary condition. Also, polynomial shape function was not regarded. Considering the ease in mathematical manipulation, applying the polynomial expression as the deflection function simplifies buckling analysis.

Onyeka *et al.* [14] used the variation energy approach in a 3D buckling analysis of a one edge clamped and other edges simply supported (CSSS) rectangular isotropic plate under compressive uniaxial load. They developed a new trigonometric shear deformation plate theory that is capable of analyzing any category of the plate. Similarly, Onyeka *et al.* [15] applied the same approach in the buckling analysis of all-edge-clamped (CCCC) isotropic thick plate with a uniaxial compressive load. However, Onyeka *et al.* [14] did not apply polynomial displacement function. Both authors did not consider a buckling analysis of 3D rectangular plates with CSFS boundary condition.

Applying a polynomial function on different thin rectangular isotropic free edge plates, inelastic buckling behavior was investigated by Eziefula [16]. Trigonometric shape function was not applied here. The stresses in the direction of thickness axis were not considered, therefore, can only predict buckling load of thin and moderately thick plates.

In the rectangular flat plates, Ezeh *et al.* [17], used polynomial displacement functions for the buckling analysis of thick plate. They assumed a shape function which can only give an approximate solution, hence, cannot be reliable in the plate's analysis as they might under-estimate the buckling load at an improved thickness of the plate. Moreso, Ezeh *et al.* [17] did not consider plate with CSFS support condition and the use of trigonometric shape function was not taken into account.

There exists an aspect of distinctiveness of the present study over the previous works put together. This includes; the method and type of analysis, type of shape functions, and plates support boundary conditions [18, 19, 20, 22]. Unlike the previous works that assumed the displacement function, the present work obtains the exact formulation from the compatibility equation to get a close form solution of the polynomial and trigonometric displacement functions. To bridge the gap in the reviewed literatures, the focus of this study is on the application of both polynomial and trigonometric shape function in analyzing the buckling behavior of a thick rectangular plate. This study will evaluate the effect of aspect ratio of the critical buckling load of a thick rectangular plate clamped on the first edge, free at the third edge, with the second and fourth edges simply supported respectively (CSFS) using a 3-D elastic plate theory.

3.0 METHODOLOGY

3.1 Potential Energy Equation Formulation

The energy equation for an axially loaded rectangular thick plate is formulated by considering a thick plate assumption, with the x-z section and y-z section,

which are initially normal to the x-y plane before bending off the normal to the x-y plane after bending of the plate as shown in the section of plate presented in the Figure 1.

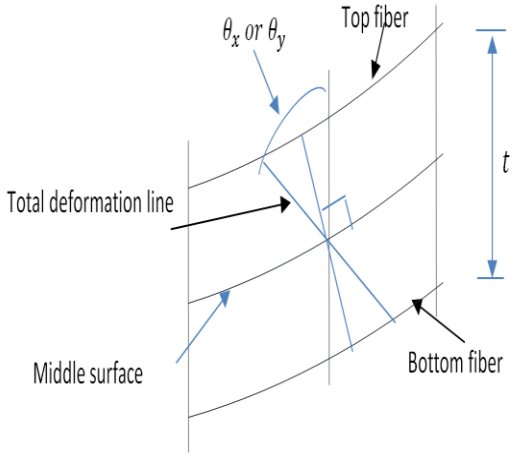

Fig. 1: Rotation of x-z (or y-z) section after bending

The non-dimensional total potential energy [∏] expression for an elastic three-dimensional plate theory of R and Q coordinates at the span-thickness aspect ratio (a/t) is in line with [14] and presented as:

$$\prod = \mathrm{D}^{*}\frac{(1-\mu)ab}{2\mathrm{a}^2(1-2\mu)}\int_0^1\int_0^1\left[(1-\mu)\left(\frac{\partial\theta_{sx}}{\partial R}\right)^2 + \frac{1}{\beta}\frac{\partial\theta_{sx}}{\partial R}\cdot\frac{\partial\theta_{sy}}{\partial Q} + \frac{(1-\mu)}{\beta^2}\left(\frac{\partial\theta_{sy}}{\partial Q}\right)^2 + \frac{(1-2\mu)}{2\beta^2}\left(\frac{\partial\theta_{sx}}{\partial Q}\right)^2 + \frac{(1-2\mu)}{2}\left(\frac{\partial\theta_{sy}}{\partial R}\right)^2 + \frac{6(1-2\mu)}{\mathrm{t}^2}\left(\mathrm{a}^2{\theta_{sx}}^2 + \mathrm{a}^2{\theta_{sy}}^2 + \left(\frac{\partial \mathrm{w}}{\partial R}\right)^2 + \frac{1}{\beta^2}\left(\frac{\partial \mathrm{w}}{\partial Q}\right)^2 + 2\mathrm{a}.\theta_{sx}\frac{\partial \mathrm{w}}{\partial R} + \frac{2\mathrm{a}.\theta_{sy}}{\beta}\frac{\partial \mathrm{w}}{\partial Q}\right) + \frac{(1-\mu)\mathrm{a}^2}{t^4}\left(\frac{\partial \mathrm{w}}{\partial S}\right)^2 - \frac{\mathrm{N_x}}{\mathrm{D}^{*}}\cdot\left(\frac{\partial \mathrm{w}}{\partial R}\right)^2\right]\partial R\partial Q \quad (1)$$

Given that D^* is the Rigidity for 3-D thick plate, let

$$D^* = D\,\frac{(1-\mu)}{(1-2\mu)}$$

Where D is the Rigidity of the CPT or incomplete 3-D thick plate, let

N_x, μ, w, θ_{Sx}, and θ_{Sy} are the uniform applied uniaxial compression load of the plate, the poison ratio, deflection , shear deformation rotation along x axis and shear deformation rotation along y axis respectively.

3.2 Compatibility Equation

The true compatibility equations in x-z plane and y-z plane according to [15] is obtained by minimizing the energy equation with respect to rotation in x-z plane and rotation in y-z plane and equate its integrands to zero to get:

$$(1-\mu)\frac{\partial^2\theta_{sx}}{\partial R^2} + \frac{1}{2\beta}\cdot\frac{\partial^2\theta_{sy}}{\partial R\partial Q} + \frac{(1-2\mu)}{2\beta^2}\frac{\partial^2\theta_{sx}}{\partial Q^2} + \frac{6(1-2\mu)}{\mathrm{t}^2}\left(\mathrm{a}^2\theta_{sx} + \mathrm{a}.\frac{\partial \mathrm{w}}{\partial R}\right) = 0 \quad (2)$$

$$\frac{1}{2\beta}\cdot\frac{\partial^2\theta_{sx}}{\partial R\partial Q} + \frac{(1-\mu)}{\beta^2}\frac{\partial^2\theta_{sy}}{\partial Q^2} + \frac{(1-2\mu)}{2}\frac{\partial^2\theta_{sy}}{\partial R^2} + \frac{6(1-2\mu)}{\mathrm{t}^2}\left(\mathrm{a}^2\theta_{sy} + \frac{\mathrm{a}.}{\beta}\frac{\partial \mathrm{w}}{\partial Q}\right) = 0 \quad (3)$$

Using the law of addition, Equations 2 and 3 will be simplified, then factorizing the outcome gives:

$$\frac{\partial w}{\partial R}\left[(1-\mu)\frac{\partial^2}{\partial R^2} + \frac{1}{\beta^2}\cdot\frac{\partial^2}{\partial Q^2}(1-\mu) + \frac{6(1-2\mu)\mathrm{a}^2}{\mathrm{t}^2}\left(1+\frac{1}{c}\right)\right] = 0 \quad (4)$$

$$\frac{1}{\beta}\cdot\frac{\partial \mathrm{w}}{\partial Q}\left[\frac{\partial^2}{\partial R^2}(1-\mu) + \frac{(1-\mu)}{\beta^2}\frac{\partial^2}{\partial Q^2} + \frac{6(1-2\mu)\mathrm{a}^2}{\mathrm{t}^2}\cdot\left(1+\frac{1}{c}\right)\right] = 0 \quad (5)$$

After simplification using law of addition, one of the possible of Equation becomes:

$$\frac{6(1-2\mu)(1+c)}{\mathrm{t}^2} = -\frac{\mathrm{c}(1-\mu)}{\mathrm{a}^2}\left(\frac{\partial^2}{\partial R^2} + \frac{1}{\beta^2}\frac{\partial^2}{\partial Q^2}\right) \quad (6)$$

3.3 General Governing Equation

The minimization of energy equation with respect to deflection gives the general governing equation as presented in [21]:

$$\frac{D^*}{2a^2}\int_0^1\int_0^1\left[\frac{6(1-2\mu)(1+c)}{t^2}\left(\frac{\partial^2 w}{\partial R^2}+\frac{1}{\beta^2}.\frac{\partial^2 w}{\partial Q^2}\right)+\frac{(1-\mu)a^2}{t^4}\frac{\partial^2 w}{\partial S^2}-\frac{N_x}{D^*}.\frac{\partial^2 w}{\partial R^2}\right]dR\,dQ=0 \quad (7)$$

Substituting Equation 6 into Equation 7 and simplifying the outcome gives two governing differential equations of a 3-D rectangular plate subject to pure buckling as presented in Equation 8 and 9:

$$\frac{\partial^4 w_1}{\partial R^4}+\frac{2}{\beta^2}.\frac{\partial^4 w_1}{\partial R^2\partial Q^2}+\frac{1}{\beta^4}.\frac{\partial^4 w_1}{\partial Q^4}-\frac{N_{x1}a^4}{gD^*}.\frac{\partial^2 w_1}{\partial R^2}=0 \quad (8)$$

$$\frac{(1-\mu)a^4}{t^4}.\frac{\partial^2 w_S}{\partial S^2}-\frac{N_{xs}a^4}{D^*}.\frac{\partial^2 w_S}{\partial R^2}=0 \quad (9)$$

Thus, the trigonometric and polynomial expression for deflection derived from Equation (8) according to Onyeka *et al*. [21] is presented in Equation (10) and (11) as:

$$w=(a_0+\ a_1R+a_2\cos g_1R+a_3\sin g_1R)\times(b_0+\ b_1Q+b_2\cos g_2Q+b_3\sin g_2Q) \quad (10)$$

$$w=\Delta_0\,(a_0+\ a_1R+a_2R^2+a_3R^3+\ a_4R^4)\times(b_0+\ b_1Q+\ b_2Q^2+b_3Q^3+b_4Q^4) \quad (11)$$

Equation (10) and (11) can be re-written in line with the work of Onyeka *et al*. [20] as:

$$w=A_1h \quad (12)$$

Where:

$$A_1=\Delta_0\begin{bmatrix}a_0\\a_1\\a_2\\a_3\\a_4\end{bmatrix}.\begin{bmatrix}b_0\\b_1\\b_2\\b_3\\b_4\end{bmatrix} \quad (13)$$

$$h=(1\ \ R\ \ \cos g_1R\ \ \sin g_1R)\times(1\ Q\ \ \cos g_2Q\ \ \sin g_2Q) \quad (14)$$

$$h=[1\ \ R\ R^2\ R^3\ \ R^4].[1\ \ Q\ Q^2\ Q^3\ Q^4] \quad (15)$$

$$\theta_{sx}=\frac{A_2}{a}.\frac{\partial h}{\partial R} \quad (16)$$

$$\theta_{sy}=\frac{A_3}{a\beta}.\frac{\partial h}{\partial Q} \quad (17)$$

Given that: h is the shape function of the plate, A_1 is the coefficient of deflection A_2 and A_3 are the coefficients of shear deformation in x axis and y axis respectively.

3.4 Direct Governing Equation

By substituting Equations (12), (16) and (17) into Equation (1), the Energy equation becomes:

$$\Pi=\frac{D^*ab}{2a^4}\Bigg[(1-\mu){A_2}^2\int_0^1\int_0^1\left(\frac{\partial^2 h}{\partial R^2}\right)^2dRdQ+\frac{1}{\beta^2}\Bigg[A_2.A_3+\frac{(1-2\mu){A_2}^2}{2}+\frac{(1-2\mu){A_3}^2}{2}\Bigg]\int_0^1\int_0^1\left(\frac{\partial^2 h}{\partial R\partial Q}\right)^2+\frac{(1-\mu){A_3}^2}{\beta^4}\int_0^1\int_0^1\left(\frac{\partial^2 h}{\partial Q^2}\right)^2dRdQ+6(1-2\mu)\left(\frac{a}{t}\right)^2\Bigg(\Big[{A_2}^2+{A_1}^2+2A_1A_2\Big].\int_0^1\int_0^1\left(\frac{\partial h}{\partial R}\right)^2dRdQ+\frac{1}{\beta^2}.\Big[{A_3}^2+{A_1}^2+2A_1A_3\Big].\int_0^1\int_0^1\left(\frac{\partial h}{\partial Q}\right)^2dRdQ\Bigg)-\frac{N_xa^2{A_1}^2}{D^*}.\int_0^1\int_0^1\left(\frac{\partial h}{\partial R}\right)^2dRdQ\Bigg] \quad (18)$$

Differentiating Equation (18) with respect to shear deformation coefficient (A_2 and A_3), and solve simultaneously gives:

$$A_2=\left(\frac{k_{12}k_{23}-k_{13}k_{22}}{k_{12}k_{12}-k_{11}k_{22}}\right).A_1 \quad (19)$$

$$A_3 = \left(\frac{k_{12}k_{13} - k_{11}k_{23}}{k_{12}k_{12} - k_{11}k_{22}}\right).A_1 \quad (20)$$

Let:

$$k_{11} = (1-\mu)k_{RR} + \frac{1}{2\beta^2}(1-2\mu)k_{RQ} + 6(1-2\mu)\left(\frac{a}{t}\right)^2 k_R \quad (21)$$

$$k_{21} = k_{12} = \frac{1}{2\beta^2}k_{RQ};\ k_{13} = -6(1-2\mu)\left(\frac{a}{t}\right)^2 k_R;\ k_{32} = k_{23} = -\frac{6}{\beta^2}(1-2\mu)\left(\frac{a}{t}\right)^2 k_Q \quad (22)$$

$$k_{22} = \frac{(1-\mu)}{\beta^4}k_{QQ} + \frac{1}{2\beta^2}(1-2\mu)k_{RQ} + \frac{6}{\beta^2}(1-2\mu)\left(\frac{a}{t}\right)^2 k_Q \quad (23)$$

Where:

$$k_{RR} = \int_0^1\int_0^1 \left(\frac{\partial^2 h}{\partial R^2}\right)^2 dRdQ \quad (24)$$

$$k_{RQ} = \int_0^1\int_0^1 \left(\frac{\partial^2 h}{\partial R\partial Q}\right)^2 dRdQ \quad (25)$$

$$k_{QQ} = \int_0^1\int_0^1 \left(\frac{\partial^2 h}{\partial Q^2}\right)^2 dRdQ \quad (26)$$

$$k_R = \int_0^1\int_0^1 \left(\frac{\partial h}{\partial R}\right)^2 dRdQ \quad (27)$$

$$k_Q = \int_0^1\int_0^1 \left(\frac{\partial h}{\partial Q}\right)^2 dRdQ \quad (28)$$

Differentiating Equation (18) with respect to deflection coefficient (A_1) and simplifying the outcome, an expression for the critical buckling load (N_{xcr}) is established as:

$$\frac{N_x a^2}{D^*} = 6(1-2\mu)\left(\frac{a}{t}\right)^2\left(\left[1+\left(\frac{k_{12}k_{23}-k_{13}k_{22}}{k_{12}k_{12}-k_{11}k_{22}}\right)\right] + \frac{1}{\beta^2}.\left[1+\left(\frac{k_{12}k_{13}-k_{11}k_{23}}{k_{12}k_{12}-k_{11}k_{22}}\right)\right].\frac{k_Q}{k_R}\right) \quad (29)$$

Similarly:

$$N_{xcr} = \frac{(1+\mu)Et^3}{2a^2}\left(\frac{a}{t}\right)^2\left(\left[1+\left(\frac{k_{12}k_{23}-k_{13}k_{22}}{k_{12}k_{12}-k_{11}k_{22}}\right)\right] + \frac{1}{\beta^2}.\left[1 + \left(\frac{k_{12}k_{13}-k_{11}k_{23}}{k_{12}k_{12}-k_{11}k_{22}}\right)\right].\frac{k_Q}{k_R}\right) \quad (30)$$

Where;

E is the modulus of elasticity and β represents the ratio of length and breadth of the plate.

3.5 Numerical Analysis

A problem of a rectangular thick plate that is clamped at first edge, simply supported at second and fourth edge and free of support at the third edge (CSFS) under uniaxial compressive load is presented. The trigonometric and polynomial displacement function as presented in the Equation (10) and (11) was applied to determine the value of the critical buckling load in the plate at various aspect ratios.

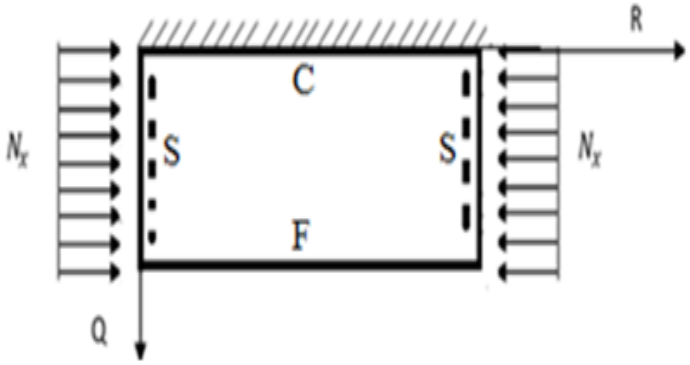

Figure 2: CSFS Rectangular Plate subjected to uniaxial compressive load

The boundary conditions of the plate in figure 3 are as follows:

At

$$R = Q = 0; \text{deflection } (w) = 0 \quad (31)$$

At

$$R = 0,\ \text{bending moment}\left(\frac{d^2w}{dR^2}\right) = 0;\ Q = 0, \text{slope}\ \left(\frac{dw}{dQ}\right) = 0 \quad (32)$$

$$\text{At}\ R = 1, \text{deflection}\ (w) = 0;\ Q = 1, \text{bending moment}\left(\frac{d^2w}{dQ^2}\right) = 0 \quad (33)$$

$$\text{At}\ R = 1, \text{bending moment}\left(\frac{d^2w}{dR^2}\right) = 0;\ \text{Q} = 1, \text{shear force}\ \left(\frac{d^3w}{dQ^3}\right) = 0 \quad (34)$$

$$\text{At Q = 1, slope}\ \left(\frac{dw}{dQ}\right) = \frac{2}{3b_5} \quad (35)$$

Substituting Equation (31) to (35) into the derivatives of w and solving gave the characteristic equation as:

$$Sin\ g_1 = 0;\ b_2 Cos\ g_1 = 0 \quad (36)$$

The value of g_1 that satisfies Equation (36) is:

$$g_1 = m\pi;\ g_1 = \frac{n\pi}{2}\ [where\ m = 1, 2, 3\ \ldots] \quad (37)$$

Substituting Equation (37) into the derivatives of w and satisfying the boundary conditions of Equation (31) to (35) gives the following constants:

$$a_1 = a_1 = a_2 = 0;\ b_1 = -g_1\ b_3 = 0;\ b_0 = -b_2 \quad (38)$$

Substituting the constants of Equation (36) and (38) into Equation (10) and simplify the outcome gives:

$$w\ = a_3 \times b_2 (Sin\ \pi R).\left(Cos\frac{n\pi Q}{2} - 1\right) \quad (39)$$

Let the amplitude,

$$A_1 = a_3 \times b_2 \quad (40)$$

And;

$$h = (Sin\ \pi R).\left(Cos\frac{\pi Q}{2} - 1\right) \quad (41)$$

Thus, the trigonometric deflection functions after satisfying the boundary conditions is:

$$w = A_1 (Sin\ \pi R).\left(Cos\frac{\pi Q}{2} - 1\right) \quad (42)$$

Similarly, substituting Equations (31 to 34) into Equation (11) and solving gives the following constants:

$$a_0 = 0;\ a_1 = 0;\ a_2 = 0;\ a_3 = -2a_4\ and \quad (43)$$

$$b_0 = 0;\ b_1 = 0;\ b_2 = 2.8b_5;\ b_3 = -5.2b_5; b_4 = 3.8b_5 \quad (44)$$

Substituting the constants of Equation (43) and (44) into Equation (11) gives;

$$w = (a_4 R - 2a_4 R^3 + a_4 R^4) \times (2.8b_5 Q^2 - 5.2b_5 Q^3 + 3.8b_5 Q^4 - b_5 Q^5) \quad (45)$$

Simplifying Equation (45) which satisfying the boundary conditions of Equation (31 to 34) gives:

$$w = a_4 (R - 2R^3 + R^4) \times b_5 (2.8Q^2 - 5.2Q^3 + 3.8Q^4 - Q^5) \quad (46)$$

Let the amplitude,

$$A_1 = a_4 \times b_5 \quad (47)$$

And;

$$h = (R - 2R^3 + R^4) \times (2.8Q^2 - 5.2Q^3 + 3.8Q^4 - Q^5) \quad (48)$$

Thus, the polynomial deflection functions after satisfying the boundary conditions is:

$$w = (R - 2R^3 + R^4) \times (2.8Q^2 - 5.2Q^3 + 3.8Q^4 - Q^5).A_1 \quad (49)$$

As such, a numerical values of the stiffness for a CSFS plate were obtained using Equation (24) to (28) by applying the two shape function (trigonometric and polynomial) as obtained in Equation (41) and Equation (48) and their results are presented in Table 1.

Table 1: The polynomial and trigonometric stiffness coefficients of deflection function of the CSFS plate

Displacement Shape Function	k_{RR}	k_{RQ}	k_{QQ}	k_R	k_Q
Polynomial	0.32848	0.09190	0.12867	0.03324	0.00931
Trigonometry	11.04427	6.08807	1.52201	1.11902	1.04191

4.0 RESULTS AND DISCUSSIONS

In this section, a numerical value of the buckling load expression obtained in Equation (29) and (30) are presented. The non-dimensional value of the critical buckling load for an isotropic rectangular plate that is clamped at first edge, simply supported at the second and fourth edge and freely support at the third edge (CSFS) under uniaxial compressive load at varying aspect ratio is presented in Table 2, 3, 4 and 5. This result was obtained by expressing the shape function of the plate in the form of trigonometry and polynomial to obtain the critical buckling load of the plate. A numerical and graphical comparison was made between the two approaches (trigonometric and polynomial functions) to study a thick plate's stability at varying thickness and aspect ratio (see table 6 and figure 3 to 11).

The values obtained in Table 2, 3, 4 and 5, shows that as the values of critical buckling load increase, the span- thickness ratio increases. This reveals that as the in-plane load on the plate increase and approaches the critical buckling, the failure in a plate structure is a bound to occur; this means that a decrease in the thickness of the plate, increases the chance of failure in a plate structure. Hence, failure tendency in the plate structure can be mitigated by increasing its thickness.

It is also observed in the tables that as the length to breadth ratio of the plate increases, the value of critical buckling load decreases while as critical buckling load increases as the length to breadth ratio increases. This implies that an increase in plate width increases the chance of failure in a plate structure. It can be deduced that as the in-plane load which will cause the plate to fail by compression increases from zero to critical buckling load, the buckling of the plate exceeds specified elastic limit thereby causing failure in the plate structure. This meant that, the load that causes the plate to deform also causes the plate material to buckle simultaneously.

The comparison shows that the present theory using trigonometric functions predicts a slightly higher value of the critical buckling load than polynomial function. This is quite expected because the trigonometric function gives higher value of stiffness coefficient than polynomial, and therefore is considered safer to use to achieve an exact three-dimensional plate analysis than polynomial displacement functions however, both provides accurate or reliable solution in the analysis of a rectangular plate.

The percentage difference of critical buckling load between the present study using polynomial, and that of trigonometric function for an isotropic CSFS thick rectangular plate subjected to a uniaxial compression at a varying aspect ratio is presented in table 6 and figures 3 to 11. It was discovered that the values of percentage error increase as the span to thickness ratio of the plate increases, the percentage differences between the two approaches reduce as the span to thickness ratio reduces. This means that as the plate gets thinner, the two methods differ more and becomes close as the plate gets thick. This shows the high level of convergence between the two approaches. It also implies a high level of accuracy and reliability in the thick plate analysis. Furthermore, the degree of the error in percentage increases as the length to breadth ratio decreases. This means that as the length of the plate widens, the two approaches (trigonometry and polynomial) become closer.

The lowest average percentage difference is 1.9144 which occurs at aspect ratio of five (5), and the highest average percentage difference is 13.3137 which occur at aspect ratio of one (1). This might indicate that in the CSFS plate the polynomial and trigonometric function converge less for the exact solution than other boundary condition (see [9] and [10]). Furthermore, the percentage difference decreases as the aspect ratio of the plate increases and decreases as the span-thickness ratio increases. This means that the thicker the plate the more the two approaches converge. It also indicates that this method is very reliable for rectangular plate analysis of any category (thin, moderately thick and thick plate).

In summary, the overall average percentage differences between the two functions recorded is 6.4%. These differences being less than 7% are quite acceptable in statistical analysis, as it will not put the structure into danger [3]. This means that at about 94% confidence both approaches are the same and can be applied with assurance for analysis of plate of any thickness. Thus, the present model has some level safety and can be used with confidence for the stability analysis of the CSFS boundary condition.

Table 2: Non-dimensional critical buckling load $\frac{N_x a^2}{Et^3}$ on the CSFS rectangular plate using polynomial function

	$N_{xcr} = \frac{N_x a^2}{\pi^2 D}$								
$\propto = \frac{a}{t}$	$\beta = 1.0$	$\beta = 1.5$	$\beta = 2.0$	$\beta = 2.5$	$\beta = 3.0$	$\beta = 3.5$	$\beta = 4.0$	$\beta = 4.5$	$\beta = 5.0$
4	1.7532	1.2606	1.1223	1.0653	1.0363	1.0195	1.0089	1.0017	0.9967
5	1.8899	1.3356	1.1838	1.1218	1.0904	1.0722	1.0608	1.0531	1.0476
10	2.1114	1.4508	1.2771	1.2072	1.1720	1.1517	1.1389	1.1303	1.1243
15	2.1586	1.4743	1.2961	1.2244	1.1884	1.1677	1.1547	1.1459	1.1397
20	2.1757	1.4828	1.3028	1.2306	1.1943	1.1734	1.1603	1.1514	1.1452
30	2.1880	1.4888	1.3077	1.2350	1.1985	1.1775	1.1643	1.1554	1.1492
40	2.1924	1.4910	1.3094	1.2366	1.2000	1.1790	1.1657	1.1568	1.1506
50	2.1944	1.4920	1.3102	1.2373	1.2007	1.1797	1.1664	1.1575	1.1512
60	2.1955	1.4925	1.3106	1.2377	1.2011	1.1800	1.1668	1.1578	1.1516
70	2.1962	1.4928	1.3109	1.2379	1.2013	1.1802	1.1670	1.1581	1.1518
80	2.1966	1.4931	1.3111	1.2381	1.2015	1.1804	1.1671	1.1582	1.1519
90	2.1969	1.4932	1.3112	1.2382	1.2016	1.1805	1.1672	1.1583	1.152
100	2.1971	1.4933	1.3113	1.2383	1.2016	1.1805	1.1673	1.1584	1.1521
1000	2.1980	1.4937	1.3116	1.2386	1.2019	1.1808	1.1676	1.1587	1.1524
1500	2.1980	1.4937	1.3116	1.2386	1.2019	1.1808	1.1676	1.1587	1.1524

Table 3: Non-dimensional Critical Buckling Load $\frac{N_x a^2}{Et^3}$ on the CSFS Rectangular Plate Using Polynomial Function

	$N_{xcr} = \frac{N_x a^2}{Et^3}$								
$\propto = \frac{a}{t}$	$\beta = 1.0$	$\beta = 1.5$	$\beta = 2.0$	$\beta = 2.5$	$\beta = 3.0$	$\beta = 3.5$	$\beta = 4.0$	$\beta = 4.5$	$\beta = 5.0$
4	1.5381	1.106	0.9846	0.9346	0.9091	0.8944	0.8851	0.8788	0.8744
5	1.6580	1.1717	1.0386	0.9842	0.9566	0.9407	0.9306	0.9239	0.9191
10	1.8523	1.2727	1.1204	1.0591	1.0282	1.0104	0.9992	0.9916	0.9863
15	1.8937	1.2934	1.1370	1.0742	1.0426	1.0244	1.0130	1.0053	0.9999
20	1.9087	1.3008	1.1430	1.0796	1.0478	1.0294	1.0179	1.0102	1.0047
30	1.9195	1.3062	1.1472	1.0835	1.0515	1.0330	1.0215	1.0137	1.0082
40	1.9234	1.3080	1.1487	1.0849	1.0528	1.0343	1.0227	1.0149	1.0094
50	1.9251	1.3089	1.1494	1.0855	1.0534	1.0349	1.0233	1.0155	1.0100
60	1.9261	1.3094	1.1498	1.0858	1.0537	1.0352	1.0236	1.0158	1.0103
70	1.9267	1.3097	1.1500	1.0860	1.0539	1.0354	1.0238	1.0160	1.0105
80	1.9271	1.3099	1.1502	1.0862	1.054	1.0355	1.0239	1.0161	1.0106
90	1.9273	1.3100	1.1503	1.0863	1.0541	1.0356	1.0240	1.0162	1.0107
100	1.9275	1.3101	1.1504	1.0863	1.0542	1.0357	1.0241	1.0162	1.0107
1000	1.9283	1.3105	1.1507	1.0866	1.0545	1.0360	1.0243	1.0165	1.0110
1500	1.9283	1.3105	1.1507	1.0866	1.0545	1.0360	1.0243	1.0165	1.0110

Table 4: Non-dimensional critical buckling load $\frac{N_x a^2}{\pi^2 D}$ on the CSFS rectangular plate using trigonometric function

$$N_{xcr} = \frac{N_x a^2}{\pi^2 D}$$

$\propto = \frac{a}{t}$	$\beta = 1.0$	$\beta = 1.5$	$\beta = 2.0$	$\beta = 2.5$	$\beta = 3.0$	$\beta = 3.5$	$\beta = 4.0$	$\beta = 4.5$	$\beta = 5.0$
4	2.1003	1.4521	1.2387	1.1423	1.0906	1.0596	1.0396	1.0259	1.0161
5	2.2340	1.5345	1.3057	1.2027	1.1474	1.1144	1.0931	1.0785	1.0681
10	2.4419	1.6602	1.4073	1.2939	1.2332	1.1970	1.1736	1.1576	1.1462
15	2.4849	1.6858	1.4279	1.3123	1.2505	1.2136	1.1898	1.1736	1.1620
20	2.5003	1.6950	1.4352	1.3189	1.2567	1.2196	1.1956	1.1792	1.1676
30	2.5114	1.7016	1.4405	1.3236	1.2611	1.2238	1.1998	1.1833	1.1716
40	2.5153	1.7039	1.4424	1.3253	1.2627	1.2253	1.2012	1.1848	1.1730
50	2.5171	1.7049	1.4432	1.3260	1.2634	1.2260	1.2019	1.1854	1.1737
60	2.5181	1.7055	1.4437	1.3265	1.2638	1.2264	1.2023	1.1858	1.1740
70	2.5187	1.7059	1.4440	1.3267	1.2641	1.2266	1.2025	1.1860	1.1743
80	2.5191	1.7061	1.4442	1.3269	1.2642	1.2268	1.2027	1.1862	1.1744
90	2.5193	1.7063	1.4443	1.3270	1.2643	1.2269	1.2028	1.1863	1.1745
100	2.5195	1.7064	1.4444	1.3271	1.2644	1.2270	1.2028	1.1863	1.1746
1000	2.5203	1.7069	1.4448	1.3274	1.2647	1.2273	1.2031	1.1866	1.1749
1500	2.5203	1.7069	1.4448	1.3274	1.2647	1.2273	1.2031	1.1866	1.1749

Table 5: Non-dimensional critical buckling load $\frac{N_x a^2}{Et^3}$ on the CSFS rectangular plate using trigonometric function

$$N_{xcr} = \frac{N_x a^2}{Et^3}$$

$\propto = \frac{a}{t}$	$\beta = 1.0$	$\beta = 1.5$	$\beta = 2.0$	$\beta = 2.5$	$\beta = 3.0$	$\beta = 3.5$	$\beta = 4.0$	$\beta = 4.5$	$\beta = 5.0$
4	1.5381	1.1060	0.9846	0.9346	0.9091	0.8944	0.8851	0.8788	0.8744
5	1.6580	1.1717	1.0386	0.9842	0.9566	0.9407	0.9306	0.9239	0.9191
10	1.8523	1.2727	1.1204	1.0591	1.0282	1.0104	0.9992	0.9916	0.9863
15	1.8937	1.2934	1.1370	1.0742	1.0426	1.0244	1.0130	1.0053	0.9999
20	1.9087	1.3008	1.1430	1.0796	1.0478	1.0294	1.0179	1.0102	1.0047
30	1.9195	1.3062	1.1472	1.0835	1.0515	1.0330	1.0215	1.0137	1.0082
40	1.9234	1.3080	1.1487	1.0849	1.0528	1.0343	1.0227	1.0149	1.0094
50	1.9251	1.3089	1.1494	1.0855	1.0534	1.0349	1.0233	1.0155	1.0100
60	1.9261	1.3094	1.1498	1.0858	1.0537	1.0352	1.0236	1.0158	1.0103
70	1.9267	1.3097	1.1500	1.0860	1.0539	1.0354	1.0238	1.0160	1.0105
80	1.9271	1.3099	1.1502	1.0862	1.0540	1.0355	1.0239	1.0161	1.0106
90	1.9273	1.3100	1.1503	1.0863	1.0541	1.0356	1.0240	1.0162	1.0107
100	1.9275	1.3101	1.1504	1.0863	1.0542	1.0357	1.0241	1.0162	1.0107
1000	1.9283	1.3105	1.1507	1.0866	1.0545	1.0360	1.0243	1.0165	1.0110
1500	1.9283	1.3105	1.1507	1.0866	1.0545	1.0360	1.0243	1.0165	1.0110

Table 6: Percentage difference of Buckling Load on the CSFS Rectangular Plate between Polynomial and trigonometry Approach

	Average Percentage Difference %								
$\propto = \frac{a}{t}$	$\beta = 1.0$	$\beta = 1.5$	$\beta = 2.0$	$\beta = 2.5$	$\beta = 3.0$	$\beta = 3.5$	$\beta = 4.0$	$\beta = 4.5$	$\beta = 5.0$
4	16.5250	13.186	9.3950	6.7425	4.9792	3.7870	2.95589	2.3583	1.91645
5	15.4049	12.961	9.3347	6.7238	4.9731	3.7848	2.95475	2.3573	1.91513
10	13.5367	12.615	9.2475	6.6992	4.9664	3.7834	2.95466	2.3570	1.91419
15	13.1304	12.544	9.2304	6.6946	4.9654	3.7835	2.95485	2.3571	1.91414
20	12.9830	12.519	9.2243	6.6931	4.9651	3.7835	2.95494	2.3572	1.91413
30	12.8759	12.501	9.2199	6.6919	4.9649	3.7835	2.95500	2.3572	1.91413
40	12.8381	12.494	9.2184	6.6915	4.9648	3.7835	2.95503	2.3572	1.91413
50	12.8205	12.491	9.2177	6.6914	4.9648	3.7835	2.95504	2.3572	1.91413
60	12.8109	12.490	9.2173	6.6913	4.9647	3.7835	2.95504	2.3572	1.91413
70	12.8052	12.489	9.2171	6.6912	4.9647	3.7835	2.95505	2.3572	1.91413
80	12.8014	12.488	9.2169	6.6912	4.9647	3.7835	2.95505	2.3572	1.91413
90	12.7988	12.488	9.2168	6.6911	4.9647	3.7835	2.95505	2.3572	1.91413
100	12.7970	12.487	9.2168	6.6911	4.9647	3.7835	2.95505	2.3572	1.91413
1000	12.7892	12.486	9.2164	6.6910	4.9647	3.7835	2.95506	2.3572	1.91413
1500	12.7892	12.486	9.2164	6.6910	4.9647	3.7835	2.95506	2.3572	1.91413
Average % difference	13.3137	12.582	9.2404	6.6977	4.9664	3.7838	2.95503	2.3573	1.9144
Total Average % difference					6.4234				

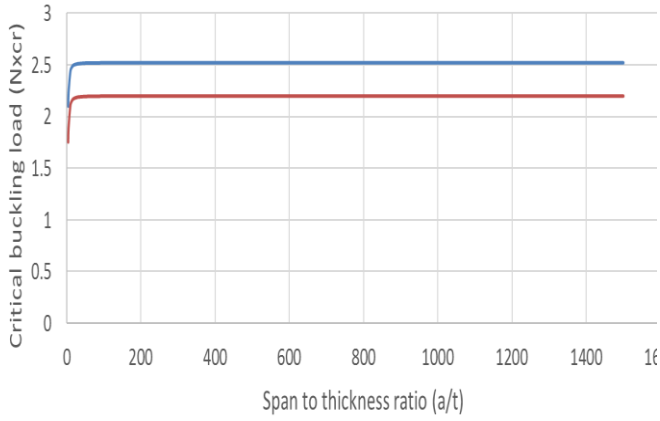

Figure 3: Critical buckling load (N_{xcr}) versus aspect ratio (a/t) of a square rectangular plate

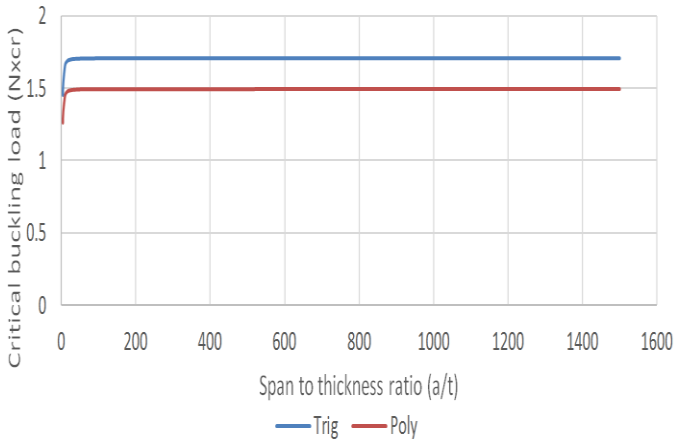

Figure 4: Critical buckling load (N_{xcr}) versus aspect ratio (a/t) of a rectangular plate with length to width ratio of 1.5.

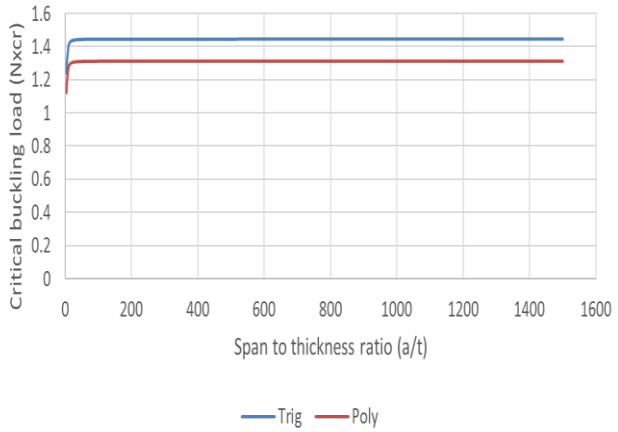

Figure 5: Critical buckling load (N_{xcr}) versus aspect ratio (a/t) of a rectangular plate with length to width ratio of 2.0

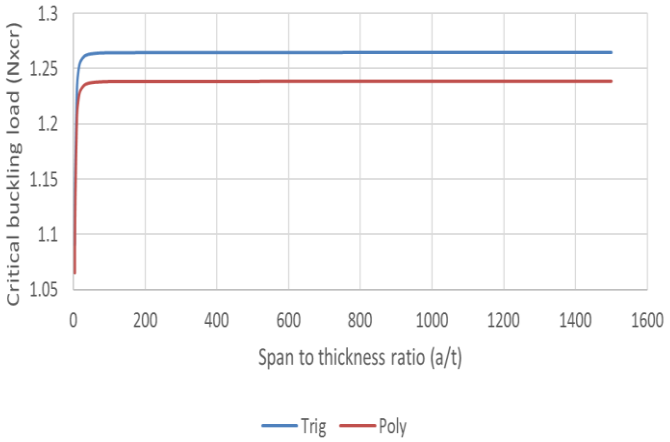

Figure 6: Critical buckling load (N_{xcr}) versus aspect ratio (a/t) of a rectangular plate with length to width ratio of 2.5

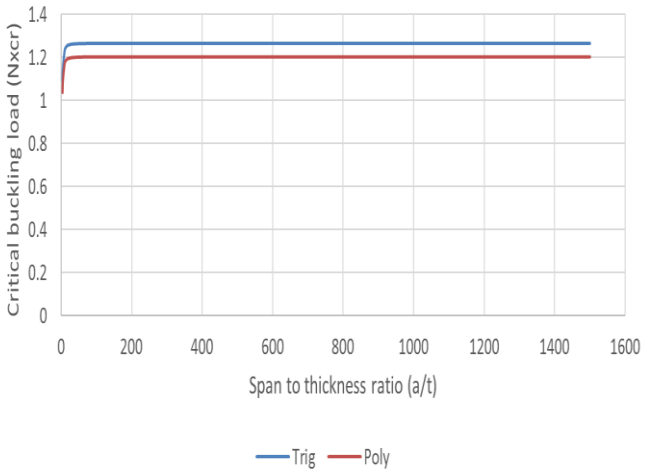

Figure 7: Critical buckling load (N_{xcr}) versus aspect ratio (a/t) of a rectangular plate with length to width ratio of 3.0

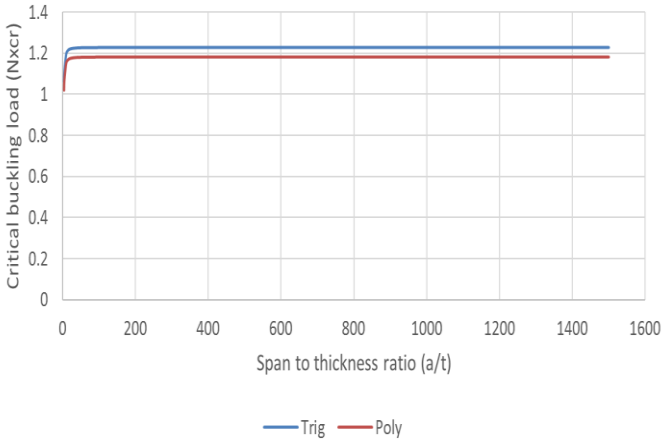

Figure 8: Graph of Critical buckling load (N_{xcr}) versus aspect ratio (a/t) of a rectangular plate with length to width ratio of 3.5

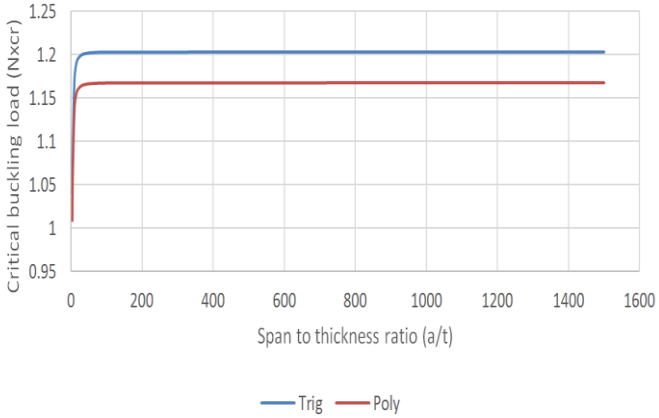

Figure 9: Critical buckling load (N_{xcr}) versus aspect ratio (a/t) of a rectangular plate with length to width ratio of 4.0

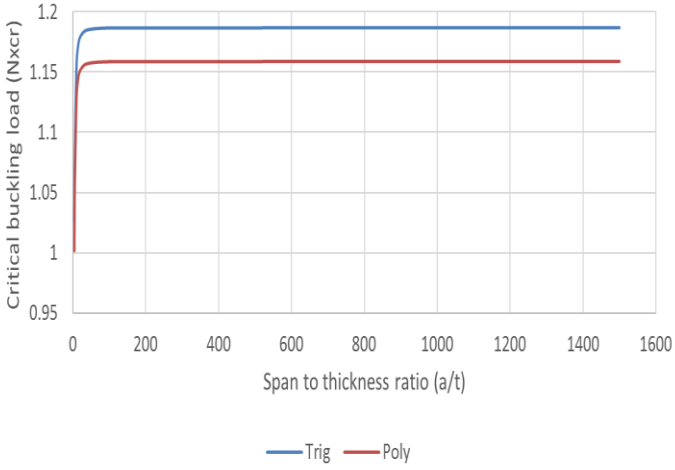

Figure 10: Critical buckling load (N_{xcr}) versus aspect ratio (a/t) of a rectangular plate with length to width ratio of 4.5

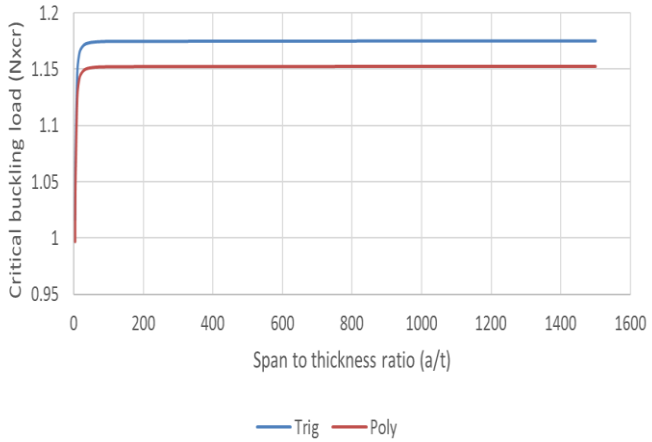

Figure 11: Critical buckling load (N_{xcr}) versus aspect ratio (a/t) of a rectangular plate with length to width ratio of 5.0

5.0 CONCLUSION AND RECOMMENDATION

From the result of this study as recorded in the percentage difference analysis, it can be concluded that the 2-D refined plate theory (RPT) is only an approximate relation for buckling analysis of thick plate [22]. More, so, the trigonometric displacement function developed to give a close form solution, thereby considered more accurate and safer for complete exact three-dimensional thick plate analysis than the polynomial. Its use in the analysis of thick plates will yield almost an exact result. On the other hand, the polynomial displacement function which predicts a slightly higher value of average percentage difference gives a close form solution whose exact value is tends to infinity. Thus, proof that the 3-D plate theory provides a reliable solution in the stability analysis of plates and can be recommended for analysis of any type of rectangular plate under support condition and load configuration.

REFERENCES

[1] Ibearugbulem, O.M. Ezeh, J.C. Ettu, L.O. "Energy Methods in Theory of Rectangular Plates (Use of Polynomial Shape Functions)," *LIU House of Excellence Ventures*, 2014.

[2] Onyeka, F.C. Osegbowa, D. and Arinze, E.E. "Application of a New Refined Shear Deformation Theory for the Analysis of Thick Rectangular Plates" *Nigerian Research Journal of Engineering and Environmental Sciences*, 5(2), 2020b, pp 901-917.

[3] Onyeka, F.C. Okeke, E.T. Wasiu, J. "Strain–Displacement Expressions and their Effect on the Deflection and Strength of Plate," *Advances in Science, Technology and Engineering Systems*, 5(5), 2020, pp 401-413. DOI: 10.25046/aj050551

[4] Onyeka, F.C. and Edozie, O.T. "Analytical Solution of Thick Rectangular Plate with Clamped and Free Support Boundary Condition Using Polynomial Shear Deformation Theory," *Advances in Science, Technology and Engineering Systems Journal*, 6(1), 2021a, pp 1427–1439. DOI: 10.25046/aj0601162

[5] Onyeka, F.C. "Direct Analysis of Critical Lateral Load in a Thick Rectangular Plate using Refined Plate Theory." *International Journal of Civil Engineering and Technology*, 10(5), 2019, pp 492-505.

[6] Onyeka, F.C. and Ibearugbulem, O.M. "Load Analysis and Bending Solutions of Rectangular Thick Plate." *International Journal on Emerging Technologies*, *11*(3), 2020, pp 1103–1110.

[7] Ezeh J.C. Ibearugbulem, O.M. Opara H. E. Oguaghamba, O.A. "Galerkin's Indirect Variational Method in Elastic Stability Analysis of all Edges Clamped Thin Rectangular Flat Plates," *International Journal of Research in Engineering and Technology*, *3*(4), 2014, pp 674-679. doi:10.15623/ijret.2014.0304119

[8] Onyeyili, I. O. "*Lecture Notes on Advanced Theory of Plates and Shells*." FUTO, (2012), SPGS.

[9] Iyengar, N. G. "*Structural Stability of Columns and Plates*." New York, (1988), Ellis Horwood Limited.

[10] Onyia, M. E., Rowland, E.O. and Ike, C. C. "Elastic Buckling Analysis of SSCF and SSSS Rectangular Thin Plates using the Single Finite Fourier Sine Integral Transform Method," *International Journal of Engineering Research and Technology*, *13*(6), (2020), pp 1147-1158. doi:10.37624/ijert/13.6.2020.1147-1158

[11] Onwuka, D.O. Ibearugbulem, O.M. Iwuoha, S.E. Arimanwa, J.I. and Sule, S. "Buckling Analysis of Biaxially Compressed All-Round Simply Supported (SSSS) Thin Rectangular Isotropic Plates using the Galerkin's Method," *Journal of Civil Engineering Urban*, 6(1), 2016, pp 48-53.

[12] Ibearugbulem, O.M. Osadebe, N.N. Ezeh, J.C. and Onwuka, D.O. "Buckling analysis of axially compressed SSSS thin rectangular plate using Taylor-Mclaurin shape function," *International Journal of Civil and Structural Engineering*, *2*(2), (2011), pp 667-672.

[13] Sayyad, A.S. and Ghugal, Y.M. "Buckling and Free Vibration Analysis of Orthotropic Plates by Using Exponential Shear Deformation Theory," *Latin American Journal of Solids and Structures, 11(8)*, (2012), pp 1298–1314. DOI: 10.1590/s1679-78252014000800001

[14] Onyeka, F. C., Okafor, F. O., Onah, H. N. "Application of a New Trigonometric Theory in the Buckling Analysis of Three-Dimensional Thick Plate," *International Journal on Emerging Technologies, 12*(1), 2021, pp 228-240.

[15] Onyeka, F.C. Okafor, F. O. and Onah, H. N. "Buckling Solution of a Three-Dimensional Clamped Rectangular Thick Plate Using Direct Variational Method," *IOSR Journal of Mechanical and Civil Engineering (IOSR-JMCE), 18*(3 Ser. III), 2021, pp 10-22. DOI: 10.9790/1684-1803031022.

[16] Eziefula, Uchechi G. "Analysis of Inelastic Buckling of Rectangular Plates with a Free Edge Using Polynomial Deflection Functions." *International Review of Applied Sciences and Engineering, 11*(1), 2020, pp 15–21. doi:10.1556/1848.2020.00003.

[17] Ezeh, J. C., Onyechere, I. C., Ibearugbulem, O. M., Anya, U. C. and Anyaogu, L. "Buckling Analysis of Thick Rectangular Flat SSSS Plates using Polynomial Displacement Functions," *International Journal of Scientific & Engineering Research, 9*(9), 2018, pp 387-392.

[18] Onyeka, F. C., Edozie, O. T. "Application of Higher Order Shear Deformation Theory in the Analysis of thick Rectangular Plate," *International Journal on Emerging Technologies, 11*(5), 2020, pp 62–67.

[19] Ibearugbulem, O. M. and Onyeka, F. C. "Moment and Stress Analysis Solutions of Clamped Rectangular Thick Plate," *EJERS, European Journal of Engineering Research and Science*, 5(4), 2020, pp 531-534. doi.org/10.24018/ejers.2020.5.4.1898

[20] Onyeka, F. C., Mama, B. O., Okeke, T. E. "Elastic Bending Analysis Exact Solution of Plate using Alternative I Refined Plate Theory," *Nigerian Journal of Technology (NIJOTECH),* 40(6), 2021, pp *1018 –1029. http://dx.doi.org/10.4314/njt.v40i6.4*

[21] Onyeka, F.C., Mama, B.O., Okeke, T.E. "Exact Three-Dimensional Stability Analysis of Plate Using A Direct Variational Energy Method," *Civil Engineering Journal,* 8(1), (2022), pp 60–80. http://dx.doi.org/10.28991/CEJ-2022-08-01-05

[22] Onyeka, F. C. Okafor, F. O. and Onah, H. N. "Application of Exact Solution Approach in the Analysis of Thick Rectangular Plate," *International Journal of Applied Engineering Research,* 14(8), 2019, pp 2043-2057.